Supplementary Materials

Potential Associations Between Low-Level Jets and Intraseasonal and Semi-Diurnal Variations in Coastal Chlorophyll-A Over the Beibuwan Gulf, South China Sea

Shuhong Liu [1,2], Danling Tang [2], Hong Yan [3], Guicai Ning [4] and Yuanjian Yang [1,2,3,*]

1. School of Atmospheric Physics, Nanjing University of Information Science & Technology, Nanjing, 210044, China
2 Southern Marine Science and Engineering Guangdong Laboratory (Guangzhou), 511458； Guangdong Key Laboratory of Ocean Remote Sensing, South China Sea Institute of Oceanology, Chinese Academy of Sciences, Guangzhou, 510301, China
3 State Key Laboratory of Loess and Quaternary Geology, Institute of Earth Environment, Chinese Academy of Sciences, Xi'an, 710061, China
4 Institute of Environment, Energy and Sustainability, The Chinese University of Hong Kong, Hong Kong, China
* Correspondence: author: Prof. Y. Yang (yyj1985@nuist.edu.cn)

Contents

1. Text S1: Corrections and Validations of the Himawari-Derived chl-a Data

2. Text S2: Ekman Pumping

3. Text S3: The Identification of Typhoon Impact Days

4. Table and Caption

5. Figures and Captions

6. References

1. Text S1: Corrections and Validations of the Himawari-Derived chl-a Data

AHI/Himawari-8 was not originally aimed at ocean remote sensing, but at meteorological applications [1]. By comparisons between the AHI-based chl-a, in situ chl-a and MODIS chl-a, previous studies have proved that the chl-a of Himawari-8 can be used after corrections [1,2], suggesting possibility of using future geostationary satellite missions for both meteorological and ocean-color purposes. Murakami [46] find that they can increase the Signal to Noise Ratio in the chl-a estimates and decrease the difference from MODIS chl-a by averaging the original 10-min images for more than one hour, and has shown that chl-a of Himawari-8 becomes noisy at 35° or higher latitude of the winter hemisphere owing to the long path of the solar light. We used Himawari-8 hourly chl-a products, and the study area is tropical ocean, which is less affected. Iwasaki [2] used the chl-a of Himawari-8 to study the daily changes of chl-a concentration by typhoon activities, and found two obvious noises and dealt with them. We also dealt with these two kinds of noise according to Iwasaki's method.

The correction of two types of noise for the chl-a product of Himawari-8 was given as followings: First, Figure S1a shows the horizontal distribution of chl-a without any noise subtractions. It can be seen that there are two noises, one is a striping noise with an interval of about 5°, and the other is a spikelike noise. Then deal with them according to the noise removal method in Iwasaki [2]. Since MODIS can also provide monthly chl-a products without striping noise, we fit the monthly chl-a of Himawari-8 to that of MODIS

by using the regression lines at each pixel. This study calculated the regression lines between the monthly chl-a of Himawari-8 and those of MODIS from August 2015 to December 2019 at each pixel. The horizontal distribution of chl-a after the MODIS fitting is shown in Figure S1b, basically the striping noise is removed. Finally, median filtering is used to reduce spikelike noise. The median filtering converts the value of a certain pixel to the median of 9 pixels. That is, with the target pixel as the center, the eight surrounding pixel values are sorted in order of magnitude, and their median value is selected as the value of the target pixel. In this way, the two types of noise are greatly reduced (Figure S1c).

2. Text S2: Ekman Pumping

This research requires the calculation of the upwelling (*upw*) caused by Ekman pumping. Price [70] proposed the Ekman pumping formula as follows:

$$upw = \nabla \times (\boldsymbol{\tau}/\rho f), \tag{1}$$

where f is the Coriolis parameter, ρ is the seawater density (1020kg m^{-3}), and $\boldsymbol{\tau}$ is the wind stress vector, which can be calculated as follows:

$$\boldsymbol{\tau} = \rho_a C_D |\mathbf{U_{10}}| \mathbf{U_{10}}; \tag{2}$$

$$C_D = \begin{cases} (4 - 0.6|\mathbf{U_{10}}|) \times 10^{-3} & for\ |\mathbf{U_{10}}| < 5\ m\ s^{-1}; \\ (0.737 + 0.0525|\mathbf{U_{10}}|) \times 10^{-3} & for\ 5\ m\ s^{-1} \le |\mathbf{U_{10}}| < 25 m\ s^{-1} \\ 2.05 \times 10^{-3} & for\ |\mathbf{U_{10}}| \ge 25\ m\ s^{-1} \end{cases} \tag{3}$$

where ρ_a is the air density (1.26 kg m^{-3}), C_D is the drag coefficient [4,5], and $\mathbf{U_{10}}$ is the 10-m wind vector.

3. Text S3: The Identification of Typhoon Impact Days

The impact of typhoons on ocean has been extensively studied. Typhoons can cause local vertical mixing or entrainment and upwelling, and transport cooler and high-nutrient seawater to the surface, thereby promoting an increase in the chl-a concentration and oceanic phytoplankton/primary productivity [6,7,8,9,10]. The monsoon winds and the occasionally strong wind events are the most important forces driving primary production in the central Beibu Gulf [16]. The response of the upper ocean to the typhoon will last for several days, depending on the strength of the typhoon and the duration of the strong wind or the transit time in response to the typhoon [6,11,12]. Therefore, in order to distinguish the influence of typhoon and LLJ, the before, during and after typhoon days are removed, according to the intensity and duration of the typhoon to eliminate the influence of typhoon days. The selected typhoon impact days are shown in the following Table S1. The identification of typhoon impact days are added as text S2 and table S1 in the supplementary materials.

4. Table and Caption

Table S1. The typhoons impacting the Beibuwan Gulf and their impacts periods during summertime from 2015–2019.

Year	Typhoons Name	Transit Periods	Total Impact Periods
2016	MIRINAE	7.25–7.28	7.25–8.4
	NIDA	8.1–8.2	8.1–8.5
	DIANMU	8.18–8.19	8.18–8.26
2017	TALAS	7.15–7.17	7.15–7.22
	SONCA	7.21–7.25	7.21–8.1
	HATO	8.23–8.24	8.23–8.27

	PAKHAR	8.27–8.28	8.27–8.31
	EWINIAR	6.5–6.9	6.5–6.16
2018	SON-TINH	7.18–7.25	7.18–8.1
	BEBINCA	8.12–8.17	8.12–8.24
	MUN	7.2–7.4	7.2–7.7
2019	WIPHA	7.30–8.3	7.30–8.10
	PODUL	8.28–8.30	8.28–8.31

Table S2. Mean and standard deviation (std) of chl-a concentration in each segment on low-level jet (LLJ) days and non-LLJ days in a) Region A, b) Region B and c) Region C. Region A, Region B, and Region C are the black boxes shown in Figure 4i.

chl-a concentration	**Region A**				**Region B**				**Region C**			
	LLJ		**non-LLJ**		**LLJ**		**non-LLJ**		**LLJ**		**non-LLJ**	
(mg m^{-3})	**mean**	**std**	**mean**	**std**	**mean**	**std**	**mean**	**std**	**mean**	**std**	**mean**	**std**
0~0.5	0.29	0.10	0.31	0.11	0.33	0.10	0.34	0.11	0.22	0.11	0.23	0.11
0.5~1	0.73	0.15	0.72	0.14	0.72	0.14	0.73	0.14	0.70	0.14	0.70	0.14
1~1.5	1.23	0.14	1.23	0.14	1.23	0.14	1.22	0.14	1.23	0.15	1.23	0.15
1.5~2	1.74	0.14	1.74	0.14	1.74	0.14	1.73	0.14	1.74	0.14	1.73	0.14
2~3	2.43	0.28	2.43	0.28	2.46	0.29	2.45	0.29	2.46	0.28	2.46	0.29
3~4	3.46	0.30	3.45	0.30	3.46	0.29	3.45	0.29	3.44	0.29	3.44	0.29
4~5	4.45	0.29	4.47	0.29	4.46	0.29	4.47	0.29	4.42	0.28	4.43	0.27
5~6	5.45	0.29	5.43	0.28	5.47	0.28	5.48	0.29	5.44	0.28	5.43	0.29
>=6	12.15	12.88	13.19	15.29	10.73	9.58	11.01	10.32	13.74	13.02	13.46	13.30

5. Figures and captions

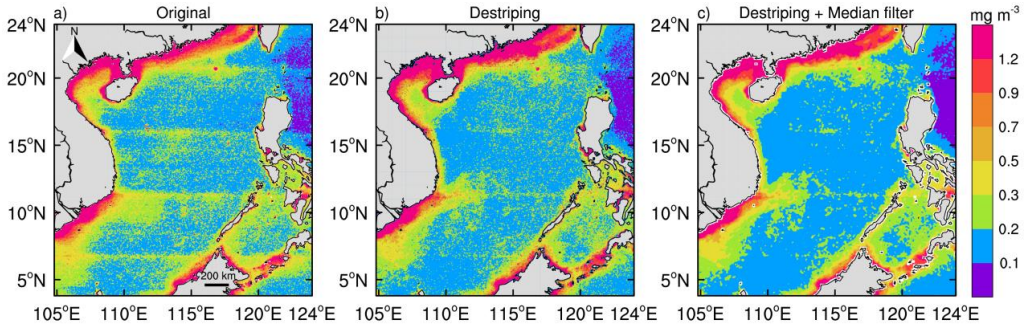

Figure S1. (**a**) Summer chl-a concentration of Himawari 8; (**b**) Same as (**a**) but with noise removed by destriping procedure; (**c**) Same as (**a**) but with noise removed by median filter and destriping procedure.

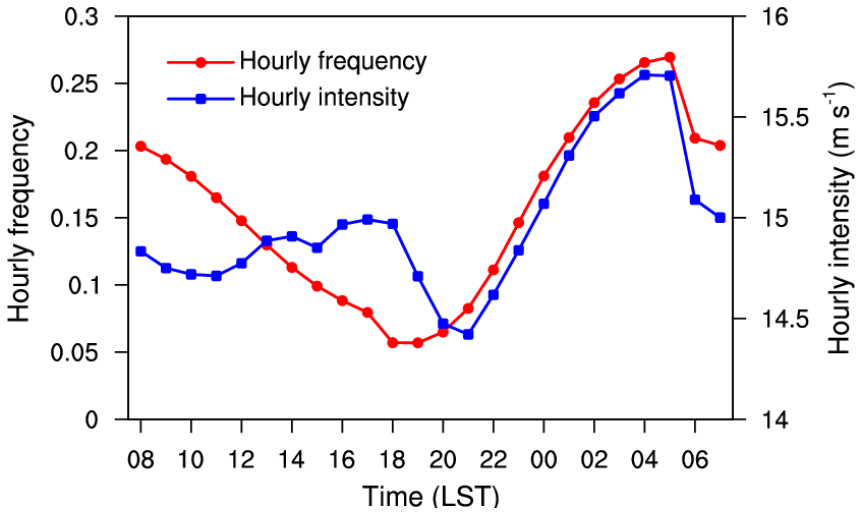

Figure S2. The hourly occurrence frequency and intensity (maximum wind speed) of LLJ over Beibuwan Gulf in summer from 2015 to 2019.

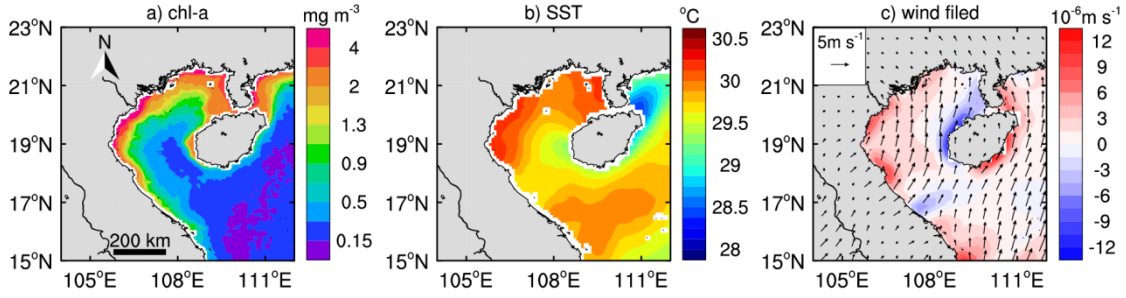

Figure S3. Average spatial distribution of (**a**) chlorophyll-a, (**b**) sea surface temperature, and (**c**) wind at 10 m (arrows) and the Ekman pumping velocity (shaded, positive value is upwelling) in summer from 2015 to 2019.

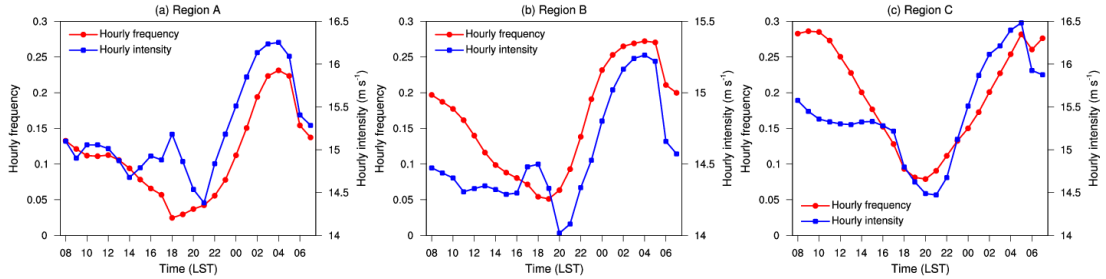

Figure S4. The hourly occurrence frequency and intensity (maximum wind speed) of LLJ over (**a**) Region A, (**b**) Region B, and (**c**) Region C in summer from 2015 to 2019. Region A, Region B, and Region C are the black boxes shown in Figure 4i.

6. References

1. Murakami, H. Ocean color estimation by Himawari-8/AHI. In Proceedings of the of SPIE Asia-Pacific Remote Sensing, New Delhi, India, 4–7 April 2016; Volume 9878, p. 987810, doi:10.1117/12.2225422.
2. Iwasaki, S. Daily Variation of Chlorophyll-A Concentration Increased by Typhoon Activity. *Remote Sens.* **2020**, *12*, 1259, doi:10.3390/rs12081259.
3. Price, J.F. Upper ocean response to a hurricane. *J. Phys. Oceanogr.* **1981**, *11*, 153–175, doi:10.1175/1520-0485(1981)011<0153:UORTAH>2.0.CO;2.
4. Jaimes, B.; Shay, L.K. Enhanced wind-driven downwelling flow in warm oceanic eddy features during the intensification of Tropical Cyclone Isaac (2012): Observations and theory. *J. Phys. Oceanogr.* **2015**, *45*, 1667–1689, doi:10.1175/JPO-D-14-0176.1.
5. Powell, M.D.; Vickery, P.J.; Reinhold, T.A. Reduced drag coefficient for high wind speeds in tropical cyclones. *Nature* **2003**, *422*, 279–283, doi:10.1038/nature01481.
6. Zheng, G.M.; Tang, D.L. Offshore and nearshore chlorophyll increases induced by typhoon winds and subsequent terrestrial rainwater runoff. *Mar. Ecol. Prog. Ser.* **2007**, *333*, 61–74, doi:10.3354/meps333061.
7. Chang, J.; Chung, C.C.; Gong, G.C. Influences of cyclones on chlorophyll a concentration and Synechococcus abundance in a subtropical western Pacific coastal ecosystem. *Mar. Ecol. Prog. Ser.* **1996**, *140*, 199–205, doi:10.3354/meps140199.

8. Yang, Y.J.; Sun, L.; Duan, A.M.; Li, Y.B.; Fu, Y.F.; Yan, Y.F.; Wang, Z.Q.; Xian, T. Impacts of the binary typhoons on upper ocean environments in November 2007. *J. Appl. Remote Sens.* **2012**, *6*, 063583, doi:10.1117/1.JRS.6.063583.
9. Zhang, S.; Xie, L.; Hou, Y.; Zhao, H.; Qi, Y.; Yi, X. Tropical storm-induced turbulent mixing and chlorophyll-a enhancement in the continental shelf southeast of Hainan Island. *J. Mar. Syst.* **2014**, *129*, 405–414, doi:10.1016/j.jmarsys.2013.09.002.
10. Zhao, H.; Han, G.; Zhang, S.; Wang, D. Two phytoplankton blooms near Luzon Strait generated by lingering Typhoon Parma. *J. Geophys. Res. Biogeosci.* **2013**, *118*, 412–421, doi:10.1002/jgrg.20041.
11. Shi, W.; Wang, M. Observations of a Hurricane Katrinainduced phytoplankton bloom in the Gulf of Mexico. *Geophys. Res. Lett.* **2007,** *34*, L11607, doi:10.1029/2007GL029724.
12. Walker, N.D.; Leben, R.R.; Balasubramanian, S. Hurricane-forced upwelling and chlorophyll a enhancement within cold-core cyclones in the Gulf of Mexico. *Geophys. Res. Lett.* **2005**, *32*, L18610, doi:10.1029/2005GL023716.